

## Challenges and opportunities for efficiency boost of next generation

### Cu(In,Ga)Se<sub>2</sub> solar cells: prospect for a paradigm shift

M. Ochoa\*, S. Buecheler, A. N. Tiwari, R. Carron

Laboratory for Thin Films and Photovoltaics, Empa-Swiss Federal Laboratories for Materials Science and Technology,  
Ueberlandstrasse 129, CH-8600 Duebendorf, Switzerland.

#### Supplementary information

##### Numerical simulation details

All numerical simulations were performed under the framework of Sentaurus workbench from Synopsys using version vP-2019.03. Drift-diffusion simulator has been used including Fermi statistics and standard models for non-radiative (S-R-H) and radiative recombination. The front and back contacts were assumed ohmic. Carrier photogeneration rate was calculated on the basis of the Transfer Matrix Method (TMM) and using AM1.5 global spectrum. A list of main material parameters is listed in Table S1.

Please have in mind that some of the material parameters listed in Table S1 have been varied. Table S1 shows the baseline parameters used for the simulations. Further details are given within the manuscript. Baseline structure (Fig. 2 within the manuscript) is composed by a layer stack of ZnO:Al (120 nm)/ZnO (40 nm)/CdS (33 nm)/CIGS (2500 nm)/Mo (500 nm).

	<b>Materials</b>			
	ZnO:Al	ZnO TCO	CdS Buffer	CIGS Absorber
<b>Band parameters</b>				
$\epsilon^{(1)}$	9	9	10	13.6
$E_g$ (eV)	3.30 <sup>(1)</sup>	3.30 <sup>(1)</sup>	2.40 <sup>(1)</sup>	1.14
$N_C$ (cm <sup>-3</sup> )	2.2·10 <sup>18</sup> (1)	2.2·10 <sup>18</sup> (1)	2.2·10 <sup>18</sup> (1)	8·10 <sup>17</sup>
$N_V$ (cm <sup>-3</sup> )	1.8·10 <sup>19</sup> (1)	1.8·10 <sup>19</sup> (1)	1.8·10 <sup>19</sup> (1)	2·10 <sup>19</sup>
<b>Doping concentration</b>				
$N_D$ (cm <sup>-3</sup> )	10 <sup>20</sup>	10 <sup>18</sup>	10 <sup>16</sup>	-
$N_A$ (cm <sup>-3</sup> )	-	-	-	10 <sup>16</sup>
<b>Band offset</b>				
$\Delta E_c$ (eV) <sup>(1)</sup>	0	-0.2		0.25
<b>Recombination parameters</b>				
$B$ (cm <sup>3</sup> /s)	1.7·10 <sup>-10</sup>	1.7·10 <sup>-10</sup>	1.7·10 <sup>-10</sup>	1.28·10 <sup>-10</sup> (2)
$\tau_p$ (ns)	0.001	0.001	0.001	-
$\tau_n$ (ns)	-	-	-	200
$S_f$ (cm/s) <sup>a</sup>	-	-	-	-
$S_b$ (cm/s) <sup>a</sup>	-	-	-	10 <sup>7</sup>
<b>Carrier mobility</b>				
$\mu_p$ (cm <sup>2</sup> /V·s)	20	25	20	100
$\mu_n$ (cm <sup>2</sup> /V·s)	50	100	50	40 <sup>(3)</sup>
<b>Optical constants</b>				
$n, k$	4	4	4	5

Table S1. List of material parameters per layer used in the simulations.  $S_b$  and  $S_f$  stand for interface recombination velocity at the front and back of each layer, respectively

For Fig. 2 in the manuscript, the CIGS absorber is graded in composition, as shown in Fig. S1a. The double graded CIGS is divided into 125 regions of 20 nm. Refractive index as a function of Ga composition is assigned to each region, as can be seen in Fig. S1b (blue curve, second right axis). Optical data for CIGS was taken from Carron et al. <sup>5</sup> as indicated in Table S1, that implements a square root dependency of the direct bandgap semiconductor and an exponential formula near and below the bandgap to account for the Urbach tails.

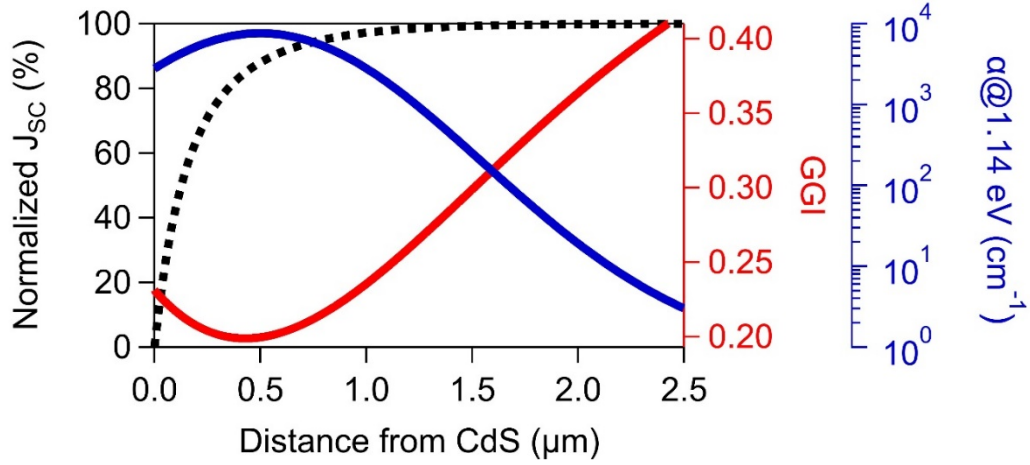


Figure S1. Normalized  $J_{sc}$  (dashed), GGI (red, first right axis) and absorption coefficient at 1.14 eV (blue, second right axis) across the absorber.

### Photon recycling modelling

We follow the model described by Steiner et al.<sup>6</sup> to quantify the main metrics for photon recycling, i.e. the average probability of re-absorption of photons ( $\overline{P_{abs}}$ ) and average probability of an emitted photon to escape out of the solar cell ( $\overline{P_{esc}}$ ). The layers of the structure are assumed planar. Material properties are considered uniform and isotropic. A TMM solver<sup>7</sup> is used to track just the intensity of light emitted and traveling inside the structure, where the degree of confinement is affected by different front and back interfaces characterized by effective Fresnel coefficients, i.e. specular effective transmission and reflection. Spontaneous emission rate is assumed uniform across the absorber. Then, the probability of re-absorption is computed integrating over all energies and angles of the spontaneous emission of light that has been absorbed, re-absorbed, emitted and re-emitted (and so on) at different locations inside the structure, via the following resulting equation of Steiner et al. model<sup>6</sup>:

$$\overline{P_{abs}} = 1 - \int_0^\infty SE(E) \times \int_0^{\frac{\pi}{2}} \left\{ \frac{1 - e^{-\alpha L / \cos\theta}}{\alpha L} \left( 1 - \frac{1}{2} (e^{-\alpha L / \cos\theta}) \left( \frac{R_f + R_b + 2R_f R_b e^{-\alpha L / \cos\theta}}{1 - R_f R_b e^{-2\alpha L / \cos\theta}} \right) \right) \right\} \cos\theta \sin\theta d\theta dE \quad (1)$$

where  $SE$  is the spontaneous emission of the absorber,  $L$  is the thickness of the absorber,  $R_f$  and  $R_b$  are the effective Fresnel coefficients at the front and the back of the structure,  $\theta$  is the angle of the photon emission with respect to the normal and  $\alpha$  the absorption coefficient of the material. We refer the reader to

reference <sup>6</sup> where the authors of the model have provided a thorough discussion and details (e.g. derivation of  $\overline{P_{esc}}$ ) about the photon recycling modelling for planar structures.

Steiner et al. model has been used to calculate  $\overline{P_{abs}}$  for different materials and structures (Fig. S2a-d). Fig. S2e shows the photon recycling factors (equivalent to  $\overline{P_{abs}}$ ) calculated by Lumb et al. <sup>8</sup> as a function of the absorber thickness for GaAs and CIGS for different back reflectors. As can be seen, good agreement is obtained for GaAs between Lumb et al. data and the one calculated in this work. Given the higher absorption coefficient for CIGS, thinner devices appear to be required to provide the same re-absorption probability than GaAs.

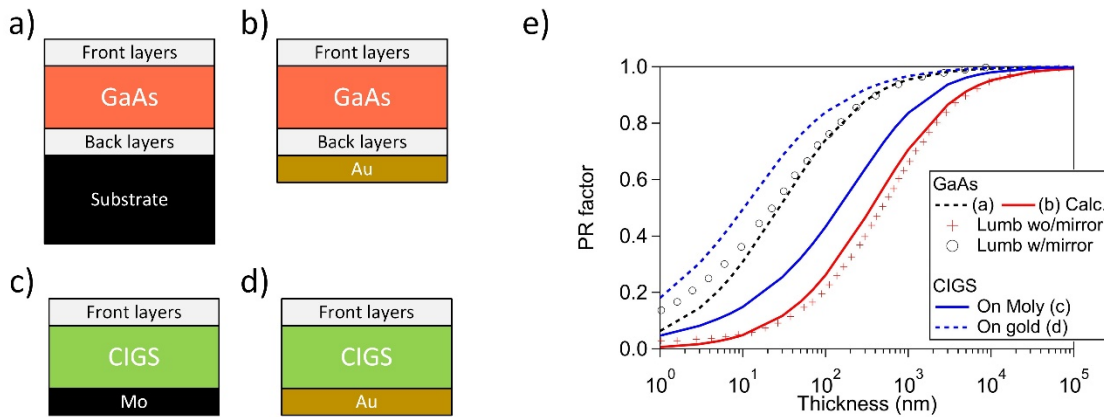


Figure S2. Layer structures simulated a)-d) and e) calculated photon recycling factors for GaAs and CIGS for different back reflectors.

### Influence of doping concentration on $V_{oc}$ including photon recycling effects

Different doping concentration were considered to expand the analysis of Fig. 4 of the manuscript. Doping levels of  $10^{15}$ ,  $10^{16}$  (baseline),  $5 \cdot 10^{16}$  and  $10^{17}$   $\text{cm}^{-3}$  were simulated.  $V_{oc}$  deficit values for each case are depicted in Fig. S3 as a function of non-radiative lifetime ( $\tau_{nr}$ ). In line with what we argue within the manuscript,  $\tau_{nr}$  must be high and/or photon recycling effects should be taken into account to explain record experimental  $V_{oc}$  deficit ( $\sim 350$  mV). For example,  $\tau_{nr} > 1 \mu\text{s}$  and  $N_A \leq 10^{16} \text{ cm}^{-3}$  are required to produce  $V_{oc}$  deficit  $\sim 350$  mV without the need to consider photon recycling effects. For higher doping cases ( $5 \cdot 10^{16}$

and  $10^{17} \text{ cm}^{-3}$ ),  $\tau_{nr}$  is in the order of hundreds of ns which is a more realistic case. In such situation, photon recycling effects cannot be neglected.

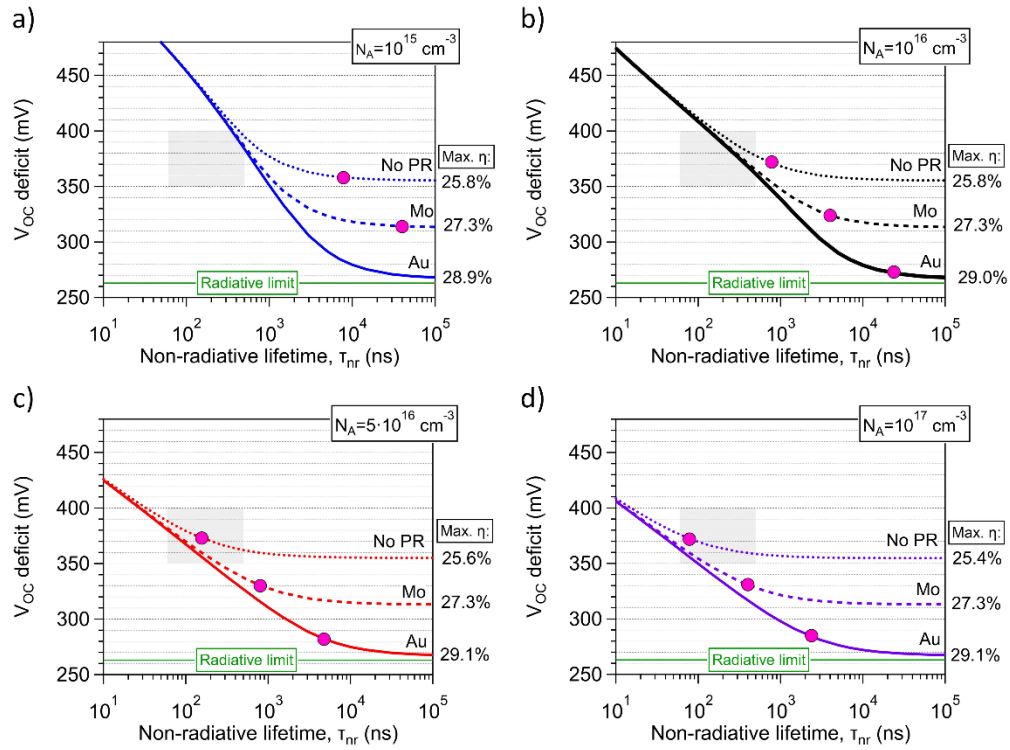


Figure S3.  $V_{oc}$  deficit as a function of non-radiative lifetime for four different absorber doping concentration: a)  $10^{15}$ , b)  $10^{16}$ , c)  $5 \cdot 10^{16}$ , d)  $10^{17} \text{ cm}^{-3}$ . The pink points depict the values where non-radiative lifetime equals the radiative lifetime. Light gray indicates the range of experimental lifetime values and  $V_{oc}$  deficit for different CIGS data. No band tails have been considered.

## References

1. Gloeckler, M., Fahrenbruch, A. L. & Sites, J. R. Numerical modeling of CIGS and CdTe solar cells: Setting the baseline. *Energy Convers.* 491–494 (2003).
2. Weiss, T. P. *et al.* Time-resolved photoluminescence on double graded Cu(In,Ga)Se<sub>2</sub> - Impact of front surface recombination and its temperature dependence. *Sci. Technol. Adv. Mater.* **20**, 313–323 (2019).
3. Weiss, T. P. *et al.* Bulk and surface recombination properties in thin film semiconductors with different surface treatments from time-resolved photoluminescence measurements. *Sci. Rep.* **9**,

5385 (2019).

4. Hara, T. *et al.* Quantitative Assessment of Optical Gain and Loss in Submicron-Textured  $\text{CuIn}_{1-x}\text{Ga}_x\text{Se}_2$  Solar Cells Fabricated by Three-Stage Coevaporation. *Phys. Rev. Appl.* **2**, 034012 (2014).
5. Carron, R. *et al.* Refractive indices of layers and optical simulations of  $\text{Cu}(\text{In,Ga})\text{Se}_2$  solar cells. *Sci. Technol. Adv. Mater.* **19**, 396–410 (2018).
6. Steiner, M. A. *et al.* Optical enhancement of the open-circuit voltage in high quality GaAs solar cells. *J. Appl. Phys.* **113**, 123109 (2013).
7. Centurioni, E. Generalized matrix method for calculation of internal light energy flux in mixed coherent and incoherent multilayers. *Appl. Opt.* **44**, 7532–7539 (2005).
8. Lumb, M. P., Steiner, M. A., Geisz, J. F. & Walters, R. J. Incorporating photon recycling into the analytical drift-diffusion model of high efficiency solar cells. *J. Appl. Phys.* **116**, 194504 (2014).